

## Theoretical Study of Au-S Interaction in Clusters Models of a $\alpha$ -cyclodextrin Complex

CARLOS ORELLANA<sup>1</sup> AND FERNANDO MENDIZABAL<sup>1\*</sup>

*1. Departamento de Química, Facultad de Ciencias, Universidad de Chile, Las Palmeras 3425, Ñuñoa, Casilla 653, Santiago, Chile.*

### ABSTRACT

Theoretical calculations were correlated to elucidate the interface interaction between thiol groups of host-guest systems and gold cluster. The 1-octanethiol molecule acts as guest into  $\alpha$ -cyclodextrin host to form a supramolecular complex in which is stabilizing gold clusters. The intermolecular interaction and the vibrational frequencies nature between a host-guest system and gold cluster were elucidated by a theoretical point of view at the MP2, SCS-MP2, and PBE-D3 methods. It is showing a van der Waals interaction and a good vibrational frequencies correlation.

**Keywords:** gold-thiol interaction, gold cluster, dispersion, frequency, theoretical calculation.

### 1. INTRODUCTION

The properties of nanomaterials arise mainly from particle size, their shape, chemical functionalization and interparticle organization. These features, in particular the interface nanoparticle with supramolecular complexes is a fascinating perspective which offers them new capabilities and functionalities [1,2]. In this regard, nanoparticles and supramolecular complexes (host-guest systems) have attracted interests for applications in molecular sensing, [3] drug delivery [4], catalysis [5] and removal of pollutants for environmental remediation, [6] because these materials achieve an efficient response at molecular level [7]. Several experimental works have pointed out the importance to develop host-guest systems with nanoparticles in a solid state to achieve practical applications [8-12]. They mentioned that when change the surrounding medium from solution to solid surface arise to switch and function including direct observation, connection with functional devices and enablement of sequential actions. One type of nano-system used to succeed these materials is gold nanoparticles (AuNPs) on solid surfaces. Gold is an inert metal, but at the "Nano" dimension it exhibits outstanding catalytic effects for important chemical transformations, [13] Plasmon bands [14], as well as their wide applications for nanostructured and biological technologies [15]. In this sense, the particle size related to chemical reactivity, inter-particle separation associated with the chemical environment are key factors that are involved in these applications.

Many techniques have been developed for directing the self-assembly of nanoparticles into ordered aggregates to achieve these features [16-19]. Ghosh et al., [20] reported that the self-assembly of nanoparticles has been of high interest to science because it provides effective building blocks for several applications. These assemblies present exciting possibilities as inter-particle separation, particle size, and particle stoichiometry may be individually manipulated to produce macroscopic solids. Creating an ordered arrangement requires a controlled self-assembly: examples include polymer surfaces [21], inorganic substrates [22-24] and single atomic monolayers [25,26]. Sada and co-workers [27] showed the first example of an anisotropic decoration of AuNPs onto the L-cystine single crystal. Further, there are reported an ordered hexagonal arrangement of metal nanoparticles (Au, Ag, Cu), controlled by self-assembly on thiol (-SH) and amine (-NH<sub>2</sub>) groups of guest molecules embedded in cyclodextrins (CD) host [28,29].

Salvarezza et al., [30] have mentioned the importance of knowledge of interface structure and the nature of the S-Au bond in molecular electronics and device fabrication. They reported that the self-assembled monolayers (SAMs) of alkanethiols on gold are key elements for building many systems and devices with applications in the wide field of nanotechnology. Also, there have been studies that suggest a non-dissociative adsorption [31,32]. In this sense, is known that its interaction is an oxidative addition, when Au surface site is bonding to R-S- through a covalent bond between them, in solution phase [33]. Gold exhibits a strong affinity for sulfur and the formation of the Au-S-R bond is feasible with a bond strength of 145-220 kJ/mol [34-37]. From a theoretical

point of view, understanding the interaction between a molecule and a nanoparticle is important for the study of various adsorption processes such as heterogeneous catalysis and monolayers on surfaces [38,39]. Accurate electronic structure calculation methods have become available. The interaction potentials of a molecule on metal are well known. The potential at short ranges, near the energy minimum is dominated by orbital interactions, i.e Pauli repulsion and covalent bonding, which require a quantum description. [40]. At longer distances, the main contribution came from electrostatic, induction and dispersion (van der Waals) interactions [41].

The adsorption of thiol compounds has been investigated on the Au (111) surface using density functional methods under the framework of the PBE (Perdew-Burke-Ernzerhof), TPSS (Tao-Perdew-Staroverov-Scuseria) and B3LYP (Becke, three-parameter, Lee-Yang-Parr) functionals [41]. The Au (111) surface was modeled using a finite-sized cluster (from Au<sub>3-26</sub>) truncated from the surface as well as a periodic slab consisting of 100 atoms [42-44]. The results reveal that the preferential adsorption site differs for the cluster models and slab approaches. The directional nature of the Au-S bond and influence of the back bond of the terminal sulfur atom are found to play key roles in the adsorption geometry. The adsorption energies suggest that the binding energies for the cluster models are weaker (van der Waals interaction) than the slab when the thiol is neutral. Moreover, in last years, it has emerged dispersion correlation to DFT (called DFT-D3) elaborated by Grimme and co-workers, which with good results for complexes [45,46] and SAMs interactions [47,48]. In this respect, our group has studied interactions between Au compounds and chalcogenides ones [49-53], which results are according with ones obtained by post-Hartree-Fock methodologies. Therefore, the DFT-D3 methodology is a good alternative to describe this kind of compounds using a low computational cost. To characterize this interaction and the chemical structure of above mentioned systems from the experimental point of view, the spectroscopic techniques offer a very important set of tools, since light provides a charge less and massless probe. Nonetheless, Raman Spectroscopy studies were missing so far in this kind of system. Two important advantages have been achieved for the use of Raman over infrared spectroscopy in the study of such S-H interactions: (i) the high intrinsic intensity of the Raman S-H stretching band and (ii) the virtual absence of spectral interference from other functional group vibrations in the Raman 2400-2700 cm<sup>-1</sup> interval [54,55].

The others complexes studied have been the  $\alpha$ -CD/C<sub>8</sub>H<sub>17</sub>SH and  $\alpha$ -CD/C<sub>8</sub>H<sub>17</sub>SH/AuNPs [53,56]. In the region 250-700 cm<sup>-1</sup>, bands for the inclusion complex were observed at 357, 435, 480, 525, 580, 600 and 613 cm<sup>-1</sup>. The first band at 357 cm<sup>-1</sup> was assigned to  $\delta$ C-S bending. However, when the supramolecular complex interacts to gold, this band shifts from 357 cm<sup>-1</sup> to 347cm<sup>-1</sup>, showing a weakening of the C-S bond. This shift is due to the interaction between S and Au, evidenced by the stretching band at 312 cm<sup>-1</sup>. The C-S stretching mode was observed at 525 cm<sup>-1</sup> for both  $\alpha$ -CD/C<sub>8</sub>H<sub>17</sub>SH and  $\alpha$ -CD/C<sub>8</sub>H<sub>17</sub>SH/AuNPs.

The authors conclude that the Au-S junction could be an intermolecular interaction rather than a covalent bond with an oxidative addition. The bands at 580, 600 and 613  $\text{cm}^{-1}$  were shifted to lower wavenumber than pure complex, which is attributed to a weakening of the S-H bond upon interaction with gold. The S-H stretching mode has been previously assigned to the band in the 2550-2580  $\text{cm}^{-1}$  region [57]. The thiol group of  $2\alpha$ -CD/ $\text{C}_8\text{H}_{17}\text{SH}$  possesses a weak intensity band at 2573  $\text{cm}^{-1}$ , attributed to moderated hydrogen bonded. The thiol stretching vibration, in a virtual absence of intermolecular hydrogen bonding, is evidenced at 2578  $\text{cm}^{-1}$ , meaning that there is a slight shift to lower wavenumber. This behavior could be due to the S atom acting as a donor as well a change in the gauche/trans configuration of the thiol in the inclusion compound. Moreover, a broad weak intensity band around 2580  $\text{cm}^{-1}$  assigned to the S-H stretching vibration was observed for  $2\alpha$ -CD/ $\text{C}_8\text{H}_{17}\text{SH}$ /AuNPs. The authors of the work conclude that sulphur is weakly hydrogen bonded, when is interacting to AuNPs. The thiol group shows a red shifting due to hydrogen bond acting as a donor (S-H $\cdots$ O) in presence of  $\alpha$ -CD or acceptor (S-H $\cdots$ AuNPs) when interacting to Au as a result polar interactions showing a shift of electron density from donor hydrogen toward its covalently bonded sulphur, yielding  $\delta$ -S-H $\delta^+$  partial charge separation.

Here we report, the theoretical elucidation of Au-S interaction on the interface between a solid supramolecular complex and gold cluster. Specifically, we achieve the description of chemical structure and interaction between  $2\alpha$ -cyclodextrin/1-octanethiol ( $2\alpha$ -CD/ $\text{C}_8\text{H}_{17}\text{SH}$ ) and gold cluster ( $\text{Au}_4$ ) by means of vibrational frequency and interaction energies theoretical calculations. The Ab initio (HF, MP2, SCS-MP2) and PBE-D3 theoretical studies were carried out in order to provide a more detailed description and some insights of the Au-SH interaction.

## 2. MATERIALS AND METHODS

Gaussian 16 package [58] has been used at the Hartree-Fock (HF), second-order Møller-Plesset perturbation theory (MP2) and SCS-MP2 (Spin-Component-Scaled) levels. Also, Turbomole v7.0 package [59], has been used for the PBE-D3 functional [60,61] that representation to electronic density of the system. The D3 correction for the DFT energy, described for Grimme et al., [40,45] was employed for the representation of the dispersion phenomena [46,62]. The following basis sets and pseudopotentials (PP) were used: the 19-valence electron (VE) quasirelativistic pseudopotential (PP) was employed for gold [63]. Two f-type polarization functions for Au atoms were employed. The f orbitals are necessary for a correct description of the intermolecular interactions, as it was demonstrated previously for various metals [64,65]. Sulphur and carbon atoms were also treated by Stuttgart pseudopotentials [66], including only the valence electrons for each atom. The double-zeta basis sets were used, augmented by d-type polarization functions; for the H atom, a triple-zeta plus one p-type polarization functions [67].

The experimental compound ( $2\alpha$ -CD/ $\text{C}_8\text{H}_{17}\text{SH}$ /AuNP) was modeled using simplified systems;  $\text{C}_8\text{H}_{17}\text{SH}$ -[Au] $_4$ ,  $\text{C}_8\text{H}_{17}\text{S}^-$ -[Au] $_4$ ,  $2\alpha$ -CD/ $\text{C}_8\text{H}_{17}\text{SH}$ -[Au] $_4$  (PBE-D3 only) and  $2\alpha$ -CD/ $\text{C}_8\text{H}_{17}\text{SH}$  (PBE-D3 only), according to experimental results [53,56]. We consider the two most important crystal planes, which were (111) and (200) to build the tip of theoretical Au cluster. According to this, the interaction of thiol group is with only one gold atom, corresponding to the (200) crystal plane, which is interacting with another 3 gold atoms from the (111) plane with an fcc packing. There are several theoretical works that describe the formation of small clusters [68] and the  $\text{Au}_4$  cluster [69]. We have used the small  $\text{Au}_4$  cluster to represent AuNPs because we can adequately described the interaction of a gold atom with  $\text{C}_8\text{H}_{17}\text{SH}$ . The main idea is to represent the interaction of a gold atom with the thiol. We have not included the cyclodextrins in models when using post-Hartree-Fock methodologies, due to size and the computational cost involved these levels of theories. To represent the complete complex, we have used the method at the PBE-D3 level. Thiolated structures were optimized on the gold cluster at HF, MP2, SCS-MP2, and PBE-D3 levels.

The counterpoise correction for the basis-set superposition error (BSSE) was used for the interaction energies calculated [70,71]. The geometry of the model, for each one of the methods mentioned above, was fully optimized. Although it is known that the MP2 approximation exaggerates the attractive interactions, this method gives a good indication of the existence of some kind of interaction [72,73]. Moreover, in order to properly quantify the Au-S interaction, we have used a modified version of the MP2 method. The method, termed SCS-MP2 (Spin-Component-Scaled) [74,75], is based on a partitioning of the correlation energy into contributions from antiparallel- $(\alpha\beta)$  and parallel-spin  $(\alpha\alpha, \beta\beta)$  pairs of electrons. This SCS-MP2 method has been used in closed-shell gold cluster and closed-shell Au(I) molecule models with results close to the CCSD(T) ones [76]. We estimate the interaction energy at the SCS-MP2 level using the equilibrium geometry of the clusters obtained at the MP2 level.

The vibrational frequencies and force constants were computed by determining the second derivatives of the energy with respect to the Cartesian nuclear coordinates from the equilibrium geometry of each model at MP2 and PBE-D3 levels as appropriate. In particular, our attention was focused on the Au-S stretching and S-H vibrational frequencies.

## 3. RESULTS AND DISCUSSION

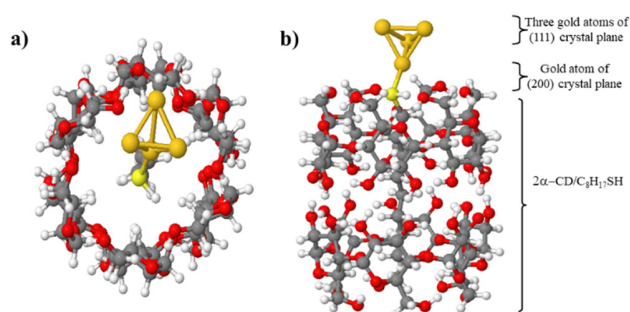
The models are divided into two sets:  $\text{C}_8\text{H}_{17}\text{SH}$ -[Au] $_4$  and  $2\alpha$ -CD/ $\text{C}_8\text{H}_{17}\text{SH}$ -[Au] $_4$  (see Fig. 1 (a) and (b)) which are neutral; and  $\text{C}_8\text{H}_{17}\text{S}^-$ -[Au] $_4$  and  $2\alpha$ -CD/ $\text{C}_8\text{H}_{17}\text{S}^-$ -[Au] $_4$ , where the thiol is anionic. The theoretical results showed that the different structural parameters change substantially when they are compared at the HF, MP2 and PBE-D3 levels (see Table 1). The Au-S distances and Au-S-C angles are significantly shortened for the MP2 and PBE-D3 methods. This provides an idea of the contribution of the electronic correlation to the intermolecular contacts for these clusters. Since it has been suggested that gold-sulfur attraction is primarily a correlation effect [77,78], the HF calculations provide a convenient way of turning off the attraction.

**Table 1.** Main geometric parameters of the systems. Distances in pm and angles in degrees.

System	Method	AuS	SH	SC	CH	AuSC	HCS	HSau
$\text{C}_8\text{H}_{17}\text{SH}$ -[Au] $_4$	HF	246.9	133.7	184.8	109.1	107.9	106.2	102.7
	MP2	228.5	135.6	186.1	110.1	101.9	105.9	100.1
	PBE-D3	234.7	136.4	186.1	109.5	108.4	108.0	100.6
$\text{C}_8\text{H}_{17}\text{S}^-$ -[Au] $_4$	HF	238.9		183.6	109.2	104.9	108.6	
	MP2	225.9		185.2	110.1	99.1	108.2	
	PBE-D3	230.3		185.0	109.8	106.0	108.7	
$2\alpha$ -CD/ $\text{C}_8\text{H}_{17}\text{SH}$ -[Au] $_4$	PBE-D3	236.0	138.0	185.1	109.6	113.0	108.0	103.2
$2\alpha$ -CD/ $\text{C}_8\text{H}_{17}\text{S}^-$ -[Au] $_4$	PBE-D3	232.3		184.3	109.5	112.5	107.8	

The  $\text{C}_8\text{H}_{17}\text{SH}$  interact with the gold cluster surface adopting an Au top-site conformation, where the S atom was located over one Au atom. The resulting S-Au bond was completely normal to the surface with a length of between 246.9 and 228.5 pm from HF to MP2, respectively, with value intermedio by PBE-D3. Thus, it is possible to infer that the bond distances are similar pointing out that the nature of the methods on the conformation of the model or the HS-Au bond distance. All the obtained conformations are in agreement with previously reported S-Au bond distances and conformations for alkanethiols [79].

When we used the complete model,  $2\alpha$ -CD/ $\text{C}_8\text{H}_{17}\text{SH}$ -[Au] $_4$ , at the PBE-D3 level the geometry is maintained without changing the geometric parameters except for the AuS and SH distances that are slightly lengthened. On the other hands, the anionic  $\text{C}_8\text{H}_{17}\text{S}^-$  is used the AuS distance reduced the magnitude all methods due to the ionic effect of the organic molecule by deprotonating the thiol group. This effect will have a substantial change in the magnitudes of the interaction energies.

**Figure 1.** Optimized structures of pure  $2\alpha$ -CD/ $C_8H_{17}SH$  and interacting to Au cluster (a and b) in balls and sticks model.

The thiol with and without proton is compared binding to gold, hence, we have carried out a comparative study of the S–Au bond strength between neutral and deprotonated sulfur models systems in their anionic form with a detailed description of the nature of this interaction. There is a strong change in the gold-sulfur distance and interaction energy when going from HF to MP2 or DFT-D3. Thus, interaction in the neutral models is dominated by van der Waals forces. See Table 2. For the anionic thiol models, the gold-sulfur distance at the HF level is slightly higher than the MP2 and PBE-D3 levels and the energies are in the range of ionic interactions. However, the methods generate different energies, related to dispersion-type van der Waals interactions with charge transfer. The SCS-MP2 method confirms that the Au-S interaction energy is 21-27% lower than MP2, for the models used. Our results revealed that the SH–gold interaction is mainly dispersive where the interaction energies range between 51 and 154 kJ/mol (see Table 2). The anionic S–gold interaction increases due to a strong charge transfer character, depicting interaction energies in the range of 247 to 397 kJ/mol, respectively. These results suggest that for the anionic models the binding strength can be tailored according to the electron–donor capabilities of the ligand.

**Table 2.** Optimized Au- $C_8H_{17}SH$  and Au- $C_8H_{17}S^-$  distances (pm), Re, for the system at the HF, MP2, SCS-MP2 and PBE-D3 levels. Interaction energy V(Re) in kJ/mol.

System	M method	Au-S	V (Re)
$C_8H_{17}SH - [Au]_4$	H F	246.9	-51.3
	M P2	228.5	-113.9
	SCS-M P2	228.5	-93.9
	PBE-D 3	234.7	-153.9
$C_8H_{17}S^- - [Au]_4$	H F	238.9	-247.0
	M P2	225.9	-343.2
	SCS-M P2	225.9	-319.4
	PBE-D 3	230.3	-392.2
$2\alpha$ -CD / $C_8H_{17}SH - [Au]_4$	PBE-D 3	236.0	-151.6
$2\alpha$ -CD / $C_8H_{17}S^- - [Au]_4$	PBE-D 3	232.8	-396.5

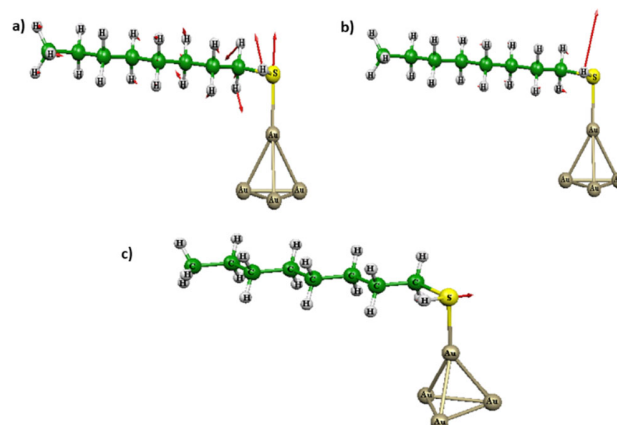
In order to confirm the effect of the neutral and anionic charge of the 1-octanethiol, we have performed a charge analysis. The charges obtained on the natural bond orbital (NBO) population on Au, S, H and C are shown in Table 3. It is easier to understand the ionic effects on the model when thiols have an anionic charge. However, a smaller charge is found at gold and sulphur in neutral models. The total charge on the gold and sulphur is of opposite sign, which permits a few ionic interactions. Moreover, the separation of charges is in agreement to the Raman spectroscopy results in the experimental [56]:  $\delta$ -S-H $\delta^+$  for the  $C_8H_{17}SH$  into an  $\alpha$ -CD host.

**Table 3.** NBO Charge on Au, S, H and C in the models  $C_8H_{17}SH-Au_4$  and  $C_8H_{17}S^- - Au_4$  at MP2 and DFT-D3 levels.

System	M ethod	Au <sub>4</sub>	Au <sup>a</sup>	S	H	C
Au <sub>4</sub>	M P2	0.000	-0.543			
	PBE-D 3	0.000	+0.222			
$C_8H_{17}SH$	M P2			-0.049	+0.111	-0.484
	PBE-D 3			-0.064	+0.122	-0.476
$C_8H_{17}S^-$	M P2			-0.748		-0.495
	PBE-D 3			-0.719		-0.504
$C_8H_{17}SH - [Au]_4$	M P2	-	-0.092	-0.069	+0.163	-0.461
	PBE-D 3	0.261 -0.205	+0.223	+0.044	+0.156	-0.473
$C_8H_{17}S^- - [Au]_4$	M P2	-	-0.068	-0.393		-0.482
	PBE-D 3	0.492 - 0.566	+0.227	-0.308		-0.497
$2\alpha$ -CD / $C_8H_{17}SH - [Au]_4$	PBE-D 3	-0.220	+0.252	+0.027	+0.187	-0.505
$2\alpha$ -CD / $C_8H_{17}S^- - [Au]_4$	PBE-D 3	-0.612	+0.234	-0.356		-0.534

<sup>a</sup>Gold atom interaction with S.

Finally, we have carried out frequency calculations on models at the MP2 and PBE-D3 levels for the ground state. Figure 2 is showing the  $\nu$ Au-S,  $\delta$ S-H and  $\nu$ S-H vibrational modes calculated by MP2 level. Table 4 shows these three frequencies for MP2 and PBE-D3 methodologies, correlated to experimental data. Furthermore, for models there are two S-H frequencies which are modified by interaction with the gold cluster when compared to free thiols. If we compare the theoretical and experimental results, the frequencies  $\nu$ Au-S at 303  $cm^{-1}$  and  $\delta$ S-H at 651  $cm^{-1}$  for PBE-D3 and the same modes for MP2 at 358  $cm^{-1}$  and 636  $cm^{-1}$  are in good agreement to the evidenced by Raman spectroscopy.

**Figure 2.** The three vibrations for thiol group, the amplitudes are exaggerated to illustrate the motion.

In addition, using model  $2\alpha$ -CD/ $C_8H_{17}SH-[Au]_4$  at the PBE-D3, we found a S-H stretching mode at 2366  $cm^{-1}$ . This value differed significantly from the experimental value at 2580  $cm^{-1}$  [53,56]. This discrepancy may be explained in terms of a change in the guest chemical environment when this is interacting to Au<sub>4</sub> cluster. In addition, the chemical environment of the guest is changing due to the presence of the  $\alpha$ -CD host, resulting in a shift to lower wavenumbers attributed to a weakening of chemical bonds. In this sense, the thiol group acts as hydrogen donor upon interaction with the gold cluster [80].

**Table 4.** Calculated harmonic frequencies (cm<sup>-1</sup>) for the models proposed systems. In parenthesis is the force constant (mdyne/Å).

System	Method	$\nu$ (S-Au)	$\nu$ (S-H)	$\nu$ (S-H)
C <sub>8</sub> H <sub>17</sub> SH	M P2		836 (0.531)	2824 (4.879)
	PBE-D3		699 (0.587)	2592 (4.116)
	Exp [54]		655	2740
C <sub>8</sub> H <sub>17</sub> SH-[Au] <sub>4</sub>	M P2	358 (0.932)	636 (0.263)	2734 (4.571)
	PBE-D3	303 (0.221)	675 (0.928)	2548 (3.977)
2 $\alpha$ -CD/C <sub>8</sub> H <sub>17</sub> SH	M P2		644 (0.501)	2622 (4.003)
	PBE-D3		663 (0.526)	2519 (4.120)
	Exp [57]		613	2573
2 $\alpha$ -CD/C <sub>8</sub> H <sub>17</sub> SH-[Au] <sub>4</sub>	PBE-D3	303 (0.220)	651 (0.492)	2366 (3.439)
2 $\alpha$ -CD/C <sub>8</sub> H <sub>17</sub> SH-[AuNP]	Exp [56]	312	605	2580

#### 4. CONCLUSIONS

This work provides new insights into the rational design and characterization of solid materials by a theoretical point of view. The Au-S interaction in the interface and an exhaustive chemical structure of a solid phase material was described by ab-initio and DFT calculations. The self-assembly is mediated by -SH functional groups, located outside the host-guest complex, evidenced through Au-S and S-H vibrational modes. Theoretical calculations allow for determination of the magnitude of the Au-S interaction, where the correlation energy plays an important role in the system stability. The theoretical results confirm that van der Waals forces predominate in the neutral systems. The estimated vibrational frequencies for Au-S and S-H are in good agreement with results obtained by vibrational and Raman spectroscopy. As a perspective, these results suggest the importance of knowing in detail the interface of Au-S systems in the solid phase for the development of new highly efficient materials in practical applications.

#### 5. ACKNOWLEDGEMENTS

The authors acknowledge FONDECYT grant 1220087 for financial support.

#### REFERENCES

1. T. Pradeep, ACS Nano. (2014), 8, 139–152.
2. L. Wenqi, L. O. Jones, W. Wu, C. L. Stern, R.A. Sponenburg, G.C. Schatz, J. F. Stoddart, J. Am. Chem. Soc. (2021), 143, 1984–1992.
3. H.N. Kim, W.X. Ren, J.S. Kim, J. Yoon, Chem. Soc. Rev. (2012), 41, 3210–3244.
4. G. Calixto, B. Fonseca-Santos, M. Chorilli, J. Bernegossi, Int. J. Nanomedicine (2014), 9, 3719–3726.
5. N. Vallavoju, J. Sivaguru, Chem. Soc. Rev. (2014), 43, 4084–4090.
6. R. Chalasani, S. Vasudevan, ACS Nano (2013), 7, 4093–4104.
7. Z. Wu, N. Song, R. Menz, B. Pingali, Y.-W. Yang, Y. Zheng, Nanomedicine (2015), 10, 1493–1514.
8. Y. Yang, Y. Sun, N. Song, Acc. Chem. Res. (2014), 47, 1950–1960.
9. K. Ariga, H. Ito, J.P. Hill, H. Tsukube, Chem. Soc. Rev. (2012), 41, 5800–5835.
10. K. Ariga, T. Mori, J.P. Hill, Soft Matter (2012), 8, 15–20.
11. A.B. Descalzo, R. Martínez-Máñez, F. Sancenón, K. Hoffmann, K. Rurack, Angew. Chemie Int. Ed. (2006), 45, 5924–5948.
12. V. Dryza, E.J. Bieske, J. Phys. Chem. C 119 (2015), 119, 14076–14084.
13. W. Huang, M. Ji, C.-D. Dong, X. Gu, L.-M. Wang, X.G. Gong, L.-S. Wang, ACS Nano (2008), 2, 897–904.
14. P.T. Bishop, L.J. Ashfield, A. Berzins, A. Boardman, V. Buche, J. Cookson, R.J. Gordon, C. Salcianu, P.A. Sutton, Gold Bull (2010), 43, 181–188.
15. [15] Z. Yang, G. Jiang, Z. Xu, S. Zhao, W. Liu, Coord. Chem. Rev. (2020), 423, 213492–213501.
16. [16] A. Badia, W. Gao, S. Singh, L. Demers, L. Cuccia, L. Reven, Langmuir (1996), 12, 1262–1269.
17. M. Möller, J.P. Spatz, A. Roescher, Adv. Mater. (1996), 8, 337–340.

18. Z. Liu, M. Frascioni, J. Lei, Z. Brown, Z. Zhu, D. Cao, J. Iehl, G. Liu, A.C. Fahrenbach, Y.Y. Botros, O.K. Farha, J.T. Hupp, C.A. Mirkin, J. F. Stoddart, Nat. Commun. (2013), 4, 1855–1860.
19. Z. Liu, A. Samanta, J. Lei, J. Sun, Y. Wang, J.F. Stoddart, J. Am. Chem. Soc. (2016), 138, 11643–11653.
20. S.K. Ghosh, T. Pal, Chem. Rev. (2007), 107, 4797–4862.
21. R. Shenhar, T.B. Norsten, V.M. Rotello, Adv. Mater. (2005), 17, 657–669.
22. M. Murugesan, D. Cunningham, J.-L. Martinez-Albertos, R.M. Vrcelj, B.D. Moore, Chem. Commun. (2005) 2677.
23. T. Shimizu, T. Teranishi, S. Hasegawa, M. Miyake, J. Phys. Chem. B. (2003), 107, 2719–2724.
24. L. Bardotti, B. Prével, P. Jensen, M. Treilleux, P. Mélinon, A. Perez, J. Gierak, G. Faini, D. Mailly, Appl. Surf. Sci. (2002), 191, 205–210.
25. S. Zhang, K.L. Chandra, C.B. Gorman, J. Am. Chem. Soc. (2007), 129, 4876–4877.
26. L. Nagle, D. Ryan, S. Cobbe, D. Fitzmaurice, Nano Lett. (2003), 3, 51–53.
27. Y. Fujiki, N. Tokunaga, S. Shinkai, K. Sada, Angew. Chemie - Int. Ed. (2006), 45, 4764–4767.
28. L. Barrientos, N. Yutronic, F. del Monte, M.C. Gutiérrez, P. Jara, New J. Chem. (2007), 31, 1400–1408.
29. L. Barrientos, P. Allende, C. Orellana, P. Jara, Inorganica Chim. Acta. (2012), 380, 372–377.
30. C. Vericat, M.E. Vela, G. Corthey, E. Pensa, E. Cortés, M.H. Fonticelli, F. Ibanez, R.C. Salvarezza, RSC Advances (53), 4, 27730–27754.
31. I.I. Rzeźnicka, J. Lee, P. Maksymowych, J.T. Yates, J. Phys. Chem. B. (2005), 109, 15992–15996.
32. M. Hasan, D. Bethell, M. Brust, J. Am. Chem. Soc. (2002), 124, 1132–1133.
33. G.A. Ozin, A.C. Arsenault, L. Cademartiri, Royal Society of Chemistry (Great Britain), Nanochemistry: a chemical approach to nanomaterials, Royal Society of Chemistry, 2009.
34. R.G. Nuzzo, B.R. Zegarski, L.H. Dubois, J. Am. Chem. Soc. (1987), 109, 733–740.
35. A. Bilić, J.R. Reimers, N.S. Hush, J. Chem. Phys. (2005), 122, 094708.
36. F.P. Cometto, P. Paredes-Olivera, V.A. Macagno, E.M. Patrino, J. Phys. Chem. B. (2005), 109, 21737–21748.
37. D.L. Kokkin, R. Zhang, T.C. Steimle, I.A. Wyse, B.W. Pearlman, T.D. Varberg, J. Phys. Chem. A. (2015), 119, 11659–11667.
38. G.-P. Brivio, M.I. Trioni, Rev. Mod. Phys. (1999), 71, 231–265.
39. G.-J. Kroes, A. Gross, E.-J. Baerends, M. Scheffler, D.A. McCormack, Acc. Chem. Res. (2002), 35, 193–200.
40. S. Grimme, J. Comput. Chem. (2006), 27, 1787–1799.
41. D. Fernández-Torre, O. Kupiainen, P. Pyykkö, L. Halonen, Chem. Phys. Lett. (2009), 471, 239–243.
42. Y. Yourdshahyan, A.M. Rappe, J. Chem. Phys. (2002), 117, 825–830.
43. D.-e. Jiang, Chem. Phys. Letters (2009), 477, 90–94.
44. P. Pyykkö, Chem. Soc. Rev. (2008), 37, 1967–1980.
45. S. Grimme, Rev. Comput. Mol. Sci. 1 (2011), 1, 211–228.
46. N. Tassinato, S. Grimme, Phys. Chem. Chem. Phys. (2015), 17, 5659–5669.
47. J. V. Koppen, M. Hapka, M. Modrzejewski, M.M. Szcześniak, G. Chałasiński, J. Chem. Phys. (2014), 140, 244313.
48. M.P. Andersson, J. Theor. Chem. 2013 (2013), 2013, 1–9.
49. S. Miranda-Rojas, R. Salazar-Molina, J. Kästner, R. Arratia-Pérez, F. Mendizábal, RSC Adv. (2016), 6, 4458–4468.
50. F. Mendizábal, S. Miranda-Rojas, L. Barrientos-Poblete, Comput. Theor. Chem. (2015), 1057, 74–79.
51. S. Miranda-Rojas, A. Muñoz-Castro, R. Arratia-Pérez, F. Mendizábal, Phys. Chem. Chem. Phys. (2013), 15, 20363.
52. A. Muñoz-Castro, T. Gomez, D.M. Carey, S. Miranda-Rojas, F. Mendizábal, J.H. Zagal, R. Arratia-Perez, J. Phys. Chem. C. (2016), 120, 7358–7364.
53. L. Barrientos, E. Lang, G. Zapata-Torres, C. Celis-Barros, C. Orellana, P. Jara, N. Yutronic, J. Mol. Model. (2013), 19, 2119–2126.
54. H. Li, G.J. Thomas, J. Am. Chem. Soc. (1991), 113, 456–462.
55. C. Rúa, M. Sepúlveda, S. Gutiérrez, J.J. Cárcamo-Vega, J. Surco-Luque, M. Campos-Vallette, F. Guzmán, P. Conti, M. Pereira, Conserv. Sci. Cult. Herit. (2017), 17, 117–137.
56. L. Barrientos, P. Allende, V. Lavayen, N. Yutronic, Private communicate. Unpublished results.

57. B.O. Skadtcenko, R. Aroca, *Acta Part A Mol. Biomol. Spectrosc.* (2001), 57, 1009–1016.
58. M.J. Frisch, G.W. Trucks, H.B. Schlegel, G.E. Scuseria, M.A. Robb, J.R. Cheeseman, J.A. Montgomery Jr., T. Vreven, K.N. Kudin, J.C. Burant, J.M. Millam, S.S. Iyengar, J. Tomasi, V. Barone, B. Mennucci, M. Cossi, G. Scalmani, N. Rega, G.A. Petersson, H. Nakatsuji, M. Hada, M. Ehara, K. Toyota, R. Fukuda, J. Hasegawa, M. Ishida, T. Nakajima, Y. Honda, O. Kitao, H. Nakai, M. Klene, X. Li, J.E. Knox, H.P. Hratchian, J.B. Cross, V. Bakken, C. Adamo, J. Jaramillo, R. Gomperts, R.E. Stratmann, O. Yazyev, A.J. Austin, R. Cammi, C. Pomelli, J.W. Ochterski, P.Y. Ayala, K. Morokuma, G.A. Voth, P. Salvador, J.J. Dannenberg, V.G. Zakrzewski, S. Dapprich, A.D. Daniels, M.C. Strain, O. Farkas, D.K. Malick, A.D. Rabuck, K. Raghavachari, J.B. Foresman, J. V Ortiz, Q. Cui, A.G. Baboul, S. Clifford, J. Cioslowski, B.B. Stefanov, G. Liu, A. Liashenko, P. Piskorz, I. Komaromi, R.L. Martin, D.J. Fox, T. Keith, M.A. Al-Laham, C.Y. Peng, A. Nanayakkara, M. Challacombe, P.M.W. Gill, B. Johnson, W. Chen, M.W. Wong, C. Gonzalez, J.A. Pople, *Gaussian Inc.*, (2016).
59. R. Ahlrichs, M. Bär, M. Häser, H. Horn, C. Kölmel, *Chem. Phys. Lett.* (1989), 162, 165–169.
60. J.P. Perdew, K. Burke, M. Ernzerhof, *Phys. Rev. Lett.* (1996), 77, 3865–3868.
61. J.P. Perdew, K. Burke, M. Ernzerhof, *Phys. Rev. Lett.* (1997), 78, 1396–1396.
62. T. Risthaus, S. Grimme, *J. Chem. Theory Comput.* (2013), 9, 1580–1591.
63. D. Andrae, U. Häußermann, M. Dolg, H. Stoll, H. Preuß, *Theor. Chim. Acta.* (1990), 77, 123–141.
64. P. Pyykkö, N. Runeberg, F. Mendizabal, *Chem. - A Eur. J.* (1997), 3, 1451–1457.
65. E.J. Fernández, A. Laguna, J.M. López-de-Luzuriaga, F. Mendizabal, M. Monge, M.E. Olmos, J. Pérez, *Chem. - A Eur. J.* (2003), 9, 456–465.
66. A. Bergner, M. Dolg, W. Küchle, H. Stoll, H. Preuß, *Mol. Phys.* (1993), 80, 1431–1441.
67. T.H. Dunning Jr., *J. Chem. Phys.* (1971), 55, 716–725.
68. P. Pyykkö, *Angew. Chemie Int. Ed.* (2004), 43, 4412–4456.
69. A.J. Pérez-Jiménez, J.C. Sancho-García, *J. Am. Chem. Soc.* 131 (2009) 14857–14867.
70. P. Hobza, R. Zahradnik, *Chem. Rev.* (1988), 88, 871–897.
71. S. Boys, F. Bernardi, *Mol. Phys.* (1970), 4, 553–566.
72. N. Runeberg, M. Schütz, H.-J. Werner, *J. Chem. Phys.* 110 (1999), 110, 7210–7216.
73. P. Pyykkö, W. Schneider, A. Bauer, A. Bayler, H. Schmidbaur, *Chem. Commun.* (1997) 1111–1112.
74. S. Grimme, *J. Chem. Phys.* (2003), 118, 9095–9102.
75. S. Grimme, *J. Comput. Chem.* (2003), 24, 1529–1537.
76. P. Pyykkö, X.-G. Xiong, J. Li, *Faraday Discuss.* (2011), 152, 169. doi:10.1039/c1fd00018g.
77. I. Ponce, J. F. Silva, R. Oñate, S. Miranda-Rojas, A. Muñoz-Castro, R. Arratia-Pérez, F. Mendizabal, J. H. Zagal, *J. Phys. Chem. C* (2011), 115, 23512–23518.
78. I. Ponce, J. F. Silva, R. Oñate, M. C. Rezende, M. A. Paez, J. H. Zagal, J. Pavez, F. Mendizabal, S. Miranda-Rojas, A. Muñoz-Castro, R. Arratia-Pérez, *J. Phys. Chem. C* (2012), 116, 15329–15341.
79. P. G. Lustemberg, M. L. Martiarena, A. E. Martínez, H. F. Busnengo, *Langmuir*, (2008), 24, 3274–3280.
80. D. Joseph, K.E. Geckeler, *Langmuir* (2009), 25, 13224–13231.